This is a repository copy of *Investigation of the Effect of a Diamine-Based Friction Modifier on Micropitting and the Properties of Tribofilms in Rolling-Sliding Contacts*.

White Rose Research Online URL for this paper:
http://eprints.whiterose.ac.uk/106162/

Version: Accepted Version

INVESTIGATION OF THE EFFECT OF A DIAMINE-BASED FRICTION MODIFIER ON MICROPITTING AND THE PROPERTIES OF TRIBOFILMS IN ROLLING-SLIDING CONTACTS

Siavash Soltanahmadi[a*], Ardian Morina[a], Marcel C. P. van Eijk[b], Ileana Nedelcu[b], and Anne Neville[a]

*s.soltanahmadi@leeds.ac.uk

[a]Institute of Functional Surfaces, School of Mechanical Engineering, University of Leeds, LS2 9JT, UK

[b]SKF Engineering and Research Centre, P.O. Box 2350, 3430 DT Nieuwegein, The Netherlands

ABSTRACT

The effect of N-Tallow-1,3-DiaminoPropane (TDP) on friction, rolling wear and micropitting has been investigated with the ultimate objective of developing lubricants with no or minimal environmental impact. A Mini Traction Machine (MTM-SLIM) has been utilised in order to generate tribofilms and observe the effect of TDP on anti-wear tribofilm formation and friction. Micropitting was induced on the surface of specimens using a MicroPitting Rig (MPR). The X-ray Photoelectron Spectroscopy (XPS) surface analytical technique has been employed to investigate the effect of TDP on the chemical composition of the tribofilm while Atomic Force Microscopy (AFM) was used to generate high resolution topographical images of the tribofilms formed on the MTM discs. Experimental and analytical results showed that TDP delays the Zinc DialkylDithioPhosphate (ZDDP) anti-wear tribofilm formation. TDP in combination with ZDDP induces a thinner and smoother anti-wear tribofilm with a modified chemical structure composed of mixed Fe/Zn (poly)phosphates. The sulphide contribution to the tribofilm and oxygen-to-phosphorous atomic concentration ratio are greater in the bulk of the tribofilm derived from a combination of TDP and ZDDP compared to a tribofilm derived from ZDDP alone. Surface analysis showed that utilising TDP effectively mitigates micropitting wear in the test conditions used in this study. Reduction of micropitting, relevant to rolling bearing applications, can be attributed to the improved running-in procedure, reduced friction, formation of a smoother tribofilm and modification of the tribofilm composition induced by TDP.

1. Introduction

Micropitting, which is encountered in bearings and gears under certain conditions, is a prevailing surface fatigue which can lead to their premature failure. The lubrication regime, type of additive package (1-6), contact pressure (7), surface roughness and topography (8, 9), and slide to roll ratio are among the factors which have influence on micropitting (4, 10). Previous studies have shown that ZDDP (1, 4) and some of the other anti-wear additives (5) can promote micropitting occurrence. Therefore, emerging additive packages which can diminish micropitting while still offering protection of the surface from wear are of great interest to industry.

Adsorption of ZDDP and its decomposition products on iron/iron-oxide surfaces has influence on the anti-wear performance of the ZDDP (11). It is assumed that a chemical interaction between the nitrogen in dispersants/amine friction modifiers and the phosphorous (12, 13) and/or the zinc (14, 15) in ZDDP can take place. While the interaction of the nitrogen in amine with phosphorous in ZDDP can be expected due to the difference in the dipole moment, the interaction of nitrogen as a complex ligand (electron-donor atom) with zinc as the coordination metal can form a metal complex which is thermodynamically stable.

The interaction of the dispersant with ZDDP induces ZDDP decomposition in oil at a lower temperature compared to ZDDP alone (16, 17). On the other hand, the assumed chemical metal complex formation in oil may lead to a reduction in the adsorption rate of ZDDP on the surface (14). Also, this chemical interaction may delay the chemisorption of ZDDP on the substrate (14, 18). As a result, the adsorption competition between free-amine and free-ZDDP and steric hindrance resulting from amine-ZDDP complex formation alter the ZDDP anti-wear properties (15, 18), while the enhanced thermo-oxidative decomposition of ZDDP can accelerate thermal film formation.

The change in the anti-wear performance of ZDDP in amine-ZDDP combination depends on the chemical structure of the nitrogen-containing molecule and its concentration in oil (14, 15). While Yamaguchi et al. (17) did not observe an alteration in the ZDDP anti-wear performance as a consequence of dispersant (as a nitrogen-containing additive) addition , Zhang et al. (19) reported an increase in the wear rate when a dispersant is introduced to the ZDDP-containing lubricant in a prolonged rubbing test.

Knowing that the nitrogen-containing additives (organic friction-modifiers and dispersants) can alter the ZDDP tribofilm properties implies that they can alter the ZDDP tribofilm that is

known to induce micropitting (1, 4). In this regard, friction modification and the affinity of the functional group of N-tallow-1,3-diaminopropane (nitrogen) to ZDDP, which brings about a delay in the ZDDP tribofilm formation and a change in the tribofilm composition (14, 18, 20), were the rationales behind studying the effect of TDP on the enhancing behavior of ZDDP on micropitting. On this basis, the aim of this study is to understand and investigate the effect of N-tallow-1,3-diaminopropane on micropitting wear, friction and tribofilm in a ZDDP-Containing lubricant.

2. Tribological experiments

2.1 Micropitting tests

Micropitting wear was investigated using a modified PCS Instruments Micropitting rig (MPR) which is schematically represented in **Figure 1** (a). The surface of interest is the surface of a spherical roller. The roller (12 mm in diameter) is in the middle and undergoes cyclic load applied by three larger and equal-diameter counterbodies which are inner rings of a cylindrical roller bearing (designation NU209) with modified roughness and outside diameter of 54.15 mm after grinding.
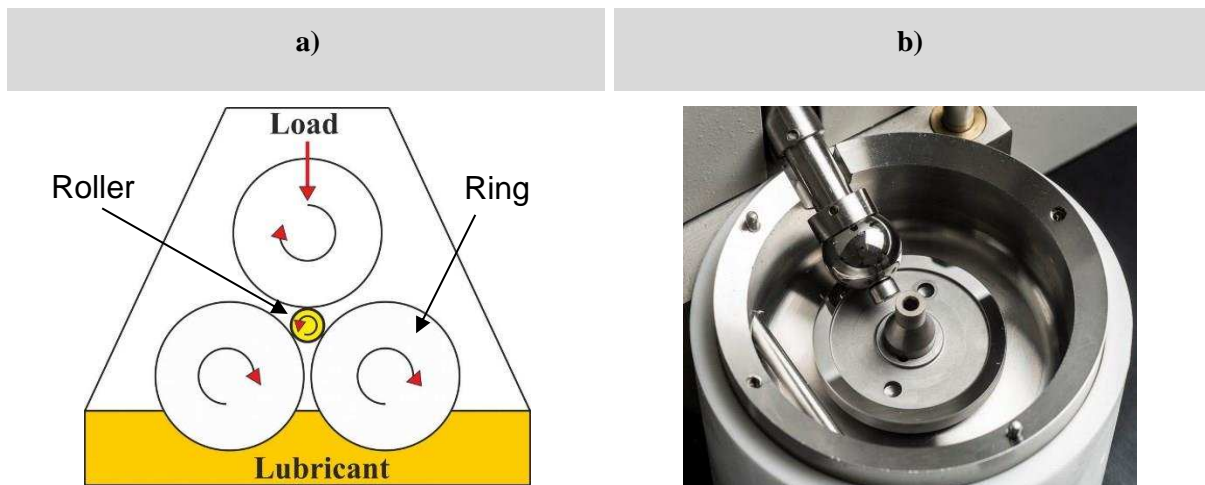
Figure 1. Schematic illustration of the test rigs a) MPR rig b) Image of the MTM pot and assemblies

In the present work rings were delicately ground-finished transverse to the rotation direction with the roughness of R_q=500±50 nm and rollers were circumferentially polished having a roughness value of R_q= 50±5 nm. Morales et al. (21) suggested that the Slide-to-Roll Ratio (SRR) of 0.01-0.02 can induce maximum surface area affected by micropitting. In this regard, the MPR experiments are carried out under two percent slide-to-roll ratio in the current study.

A transverse roughness, rather than longitudinal or isotropic, of the counterbody induces the maximum micropitting on the smoother body (1, 21). A perpendicular surface lay to the sliding direction is also thought to cause micropitting in gears (10). The experimental conditions in the present work are indicated in **Table 1**.

Table 1. MPR test parameters

Specimens	Roller: 52100 steel, R_q: 50 nm HV: 785
	Rings: 52100 steel, R_q: 500 nm, HV: 745
P_{max}	1.5 GPa
Temperature	90°C
Load cycles (on roller)	1×10^6
Slide-to-roll ratio (%)	2
Entrainment speed	1 m/s

2.2 Friction tests

The effect of TDP on the frictional properties and tribofilm formation has been investigated using a PCS Instruments MTM rolling-sliding tribometer shown in **Figure 1**(b). The experimental specimens and parameters are listed in **Table 2**.

Table 2. MTM test parameters

Specimens	Ball	Disc
Material and dimension (diameter)	AISI 52100 steel - 19.05mm	AISI 52100 steel - 46mm
Hardness (HV)	800-920	720-780
Roughness (R_a in nm)	16	8
P_{max} (GPa)	1	
Temperature (°C)	90	
Rubbing-step duration between Stribeck steps (in minute)	5, 10, 15, 30, 60, 60, 60	
Stribeck diagrams and mapping after total rubbing times of (min)	0 (initial), 5, 15, 30, 60, 120, 180, 240	
Slide-to-roll ratio (%) throughout the test	5	
Entrainment speed for all rubbing steps	100 mm/s	
Entrainment speed range for Stribeck curve	3000 – 15 mm/s	

Applying 35 N, 1 GPa of maximum Hertzian contact pressure has been applied to the surfaces at the start of the experiments. The bulk lubricant temperature was maintained and controlled at 90°C and SRR was set to 5% during all MTM experiments. Once the oil reached a steady temperature of 90°C, the load was applied and a Stribeck curve (3000–15 mm/s) was measured which is then followed by a rubbing step at a constant entrainment speed of 100 mm/s and a SRR of 5% for a pre-defined time interval. The Spacer Layer Imaging Method (SLIM) coupled with MTM was employed to map and measure the thickness of the reaction film formed on the ball surface after this rubbing step.

SLIM uses a white light source to capture the tribofilm based on the optical interferometric technique. At the end of each rubbing step, the ball was stopped and loaded in reverse against a glass window through which a static image was taken from the wear track on the ball surface using an RGB camera. The topmost surface of the glass is coated with a transparent silica space-layer, beneath which is a thin and semi-reflective chromium layer. The beams reflected from the chrome layer and the ball surface generate an interference image following recombination of the light paths. The image is frame-grabbed by the camera and analysed by the control software to determine the film thickness. SLIM has been explained in detail by Taylor et al. (22).

The three-step test procedure, based on the procedure applied by Taylor et al. (22, 23), was repeated several times during the experiment in order to understand the TDP effect on the frictional properties of the lubricant and tribofilm formation after specific rubbing time intervals. Stribeck friction curves acquired at the start of the test and then after total rubbing time of 5, 15, 30 min, 1, 2, 3 and 4 h, respectively, are plotted for the different lubricants. Each test has been repeated twice and the reported results are the average of the repeated experiments.

2.3 Lubricants

The base stock used is a low-viscosity poly-alpha-olefin (PAO) base oil. The kinematic viscosity of the base oil was 4.0 cSt at 100°C. The dynamic viscosity of the base stock which is used to calculate the minimum lubricant-film thickness in contact was 2.85 mPa.s at 90°C. Minimum film thickness in the contact ($h_{min} = H_{min} \times R_x$) has been calculated using the Hamrock-Dowson equation (24) indicated as Eq 1.

$$H_{min} = 3.63 \left(\frac{U_e \eta_0}{E' R_x}\right)^{0.68} (\alpha E')^{0.49} \left(\frac{W}{E' R_x{}^2}\right)^{-0.073} \left(1 - e^{-0.68k}\right) \quad \textbf{Equation 1.}$$

Where H $_{min}$ is minimum dimensionless film thickness, R_x $((\frac{1}{R_{x,a}} + \frac{1}{R_{x,b}})^{-1})$ is the effective radius of the curvature in the direction of x (tangent to the path of motion), $R_{x,a}$ and $R_{x,b}$ are the radius of curvature of body a (ball/roller) and body b (disc/ring) in MTM ball-on-disc and MPR roller-rings type of contact in the direction of x, respectively, α is the viscosity-pressure coefficient (1.1×10^{-8} Pa^{-1}), W is the normal load (N), U_e is the lubricant entrainment speed (m/s), η_0 is the dynamic viscosity of the lubricant (2.84×10^{-3} Pa.s), E' is the effective modulus of elasticity, and k is the elliptical parameter which is equal to 1.03 and 4.08 in MTM ball-on-disc and MPR roller-rings type of contact respectively.

Lambda ratio (λ) is the indication of the lubrication regime in the centre of contact and defined as the ratio of the minimum film thickness (h_{min}) to the average root mean square roughness of the two surfaces (Eq 2).

$$\lambda = \frac{h_{min}}{\sqrt{R_{q,a}{}^2 + R_{q,b}{}^2}} \quad \textbf{Equation 2.}$$

Where $R_{q,a}$ and $R_{q,b}$ are the root mean square roughness of the contact body one (ball/roller) and contact body two (disc/rings), respectively. The initial lambda ratio at the start of the contact was $\lambda=0.17$ and $\lambda=0.045$ in MTM tests and MPR tests respectively. Both MTM and MPR tribological tests have been carried out using four lubricants; details are given in **Table 3**:

Table 3. Lubricant formulation table

Lubricant name	Lubricant formulation	Lubricant name	Wt% Phosphorous	Wt% Nitrogen / Wt% Phosphorous
Oil-A	PAO base oil υ= 4 cSt @100°C	BO	-	-
Oil-B	PAO + ZDDP	BO+ZDDP	0.08	-
Oil-C	Oil-B + TDP at concentration of 0.5 wt%	BO+ZDDP+TDP(C)	0.08	0.55
Oil-D	Oil-B + TDP at concentration of 1.0 wt%	BO+ZDDP+TDP(2C)	0.08	1.1

The TDP additive was blended to the oils using an ultrasound bath at 45-50°C whilst mixing for 30 minutes.

3. Surface Analysis

3.1 Wear Measurement

The wear volume measurement has been carried out using a Bruker's NPFLEX based on Wyko (White Light Interferometry (WLI)) technology. Wear track profiles of three spots of each specimen have been generated and the average value of the three spots is considered as wear volume. The wear measurement has been done on the rollers used in MPR. Prior to the wear measurement, the tribofilm and residual oil on the specimen have been removed thoroughly by wiping the specimen's surface using tissue and acetone followed by ultrasonic cleaning in acetone for thirty minutes.

3.2 Optical microscopy

A Leica Stereo Microscope (M205 C) was used to capture images from the surface of the MPR rollers. Prior to the microscopy the residual oil was removed through ultrasonic cleaning in isopropanol for three minutes.

3.3 Scanning Electron Microscopy (SEM)

A Zeiss Supra 55 SEM is utilised to capture images through secondary electron detector collecting the secondary electrons emitted from the surface of the MPR rollers. The specimen's electrons have been excited by electrons coming from the electron-gun having acceleration voltage of 5 kV. The residual lubricant on the specimen has been cleaned through flushing n-heptane followed by ultrasonic cleaning in n-heptane for three minutes prior to SEM analysis.

3.4 X-ray Photoelectron Spectroscopy (XPS)

XPS surface analysis has been carried out utilising a PHI 5000 Versa Probe™ spectrometer (Ulvac-PHI Inc, Chanhassen, MN, USA) which uses a monochromatic Al Kα X-ray source (1486.6 eV).

Prior to the XPS analysis residual lubricant on the surface has been eliminated through flushing n-heptane followed by ultrasonic cleaning in n-heptane for three minutes. Survey spectra with an energy step size of 1 eV were collected from different locations in order to accurately identify inside and outside of the tribological contact. Detailed spectra have been collected from small areas inside the wear track approximately at the centre with a beam size of 100 µm×100 µm and a power of 23.7 W in the fixed analysed transmission mode selecting an energy step size of 0.05 eV for the oxygen, iron, phosphorous, and sulphur acquisition and 0.1 for carbon and zinc. The residual chamber pressure was always lower than 5×10^{-7} Pa during spectra acquisition.

The detailed XPS spectra were fitted using CASAXPS software (version 2.3.16, Casa Software Ltd, UK) with Gaussian–Lorentzian curves after subtracting a Shirley background. The

charging of the specimen has been corrected by referring aliphatic carbon binding energy to 285.0 eV (as a contamination). The curve fitting procedures for the phosphorous signal (P 2p) and the sulphur signal (S 2p) were performed applying an area-ratio-constraint of 2:1 for the two components of the signal ($p_{3/2}$ and $p_{1/2}$), in accordance with spin-orbit splitting (25). Also, position-difference-constraints of 0.85 eV and 1.25 eV are applied for the two components of the phosphorus and sulphur signals, respectively in the detailed XPS spectra fitting procedure. An Ar^+ ion source (2 keV energy, 2×2 mm^2 area and 1 µA sputter current) has been used to sputter the reaction film on the wear track in order to attain the elemental distribution of reaction film across its depth and estimate the reaction film thickness. Ion sputtering was carried out every 60 s between XPS acquisition and its rate on steel was found to be 4.5 nm per minute by Wyko. The sputtering time at which the concentration of O1s signal becomes less than 5% and no traces of the tribofilm elements (Zn, P, S) is found, is considered as a measure of the reaction layer thickness (25).

3.5 Topographical/roughness analysis of the tribofilm

AFM analysis provides nanometre-scale resolution, thus a Bruker's (Dimension Icon) AFM was used in order to study the topographical characteristics of the tribofilms formed on the MTM disc surfaces. Scans were carried out in tapping mode over areas of 20 µm × 20 µm and 5 µm × 5 µm for the tribofilm roughness and morphology study. Separate MTM tests were carried out for AFM measurements using the BO+ZDDP and BO+ZDDP+TDP(C) lubricant formulation. Test conditions are indicated in **Table 4**.

Table 4. Experimental setup for topographical AFM analysis

Specimens	52100 steel R_a: ball= 16 nm Disc: 8 nm
P_{max}	1 GPa
Temperature	90°C
Slide-to-roll ratio (%) throughout the test	5
Entrainment speed	100 mm/s
Test duration	120 minutes
AFM scanning after rubbing time of	15, 120 minutes

For the AFM study, the test is halted after 15 minutes of rubbing followed by AFM analysis of the wear track on the MTM disc while the ball remained attached to the shaft. The oil was

replaced with the fresh oil and a further rubbing step of 105 minutes was carried out on the same specimen. The second AFM scan, performed on the disc, corresponds to the tribofilm formed after two hours of rubbing in total. The AFM scans after a rubbing duration of 15 minutes and 120 minutes were selected to represent the early/middle stage of the tribofilm formation and the established stage of the tribofilm formation (at which the friction coefficient and tribofilm-thickness will remain relatively constant), respectively.

4. Results

4.1 Tribofilm thickness

The MTM tests were carried out to investigate tribofilm thickness and friction. A ZDDP tribofilm was seen to form on the surface after nearly five minutes of rubbing in the BO+ZDDP lubricant formulation. As can be seen in **Error! Reference source not found.**, for the BO+ZDDP+TDP(C) and BO+ZDDP+TDP(2C) the period was delayed to thirty minutes and one hour, respectively. The delaying effect was enhanced when the concentration of TDP was doubled. Addition of the TDP to the lubricant resulted in a 20 nm thick tribofilm, while BO+ZDDP lubricant generates a 90 nm thick tribofilm at the end of the test.
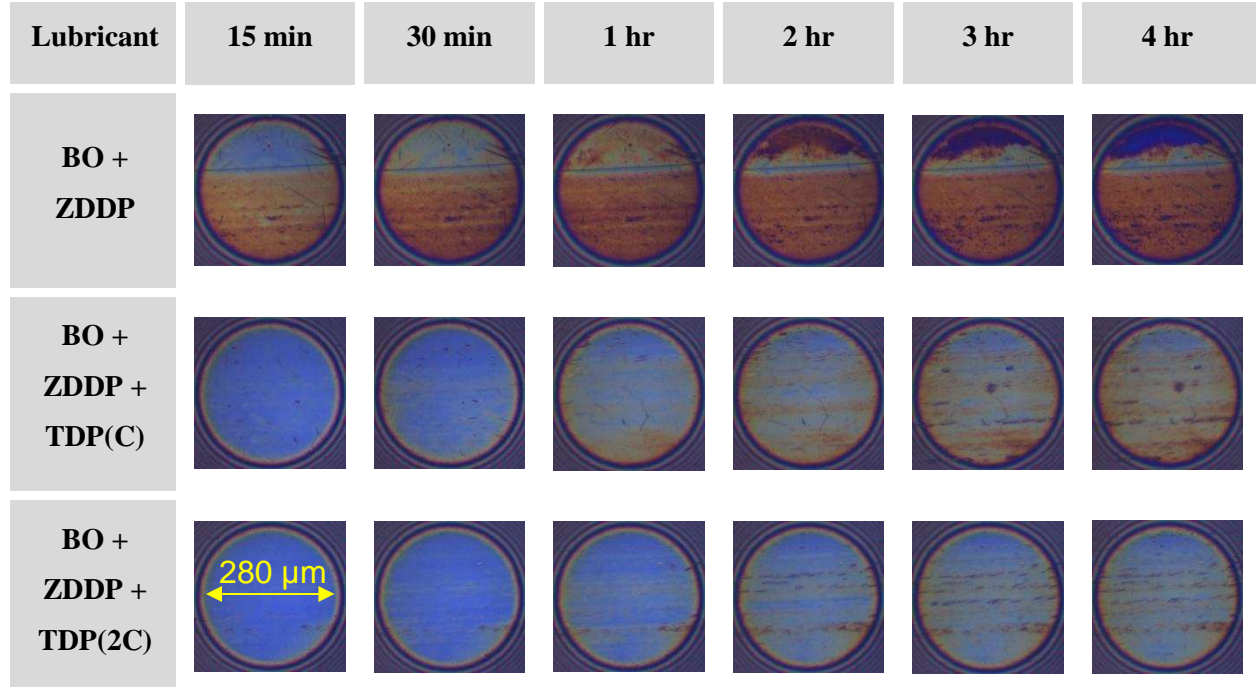

Figure 2. MTM tribofilm evolution over rubbing-time in the three lubricant formulations. The circular contact zones in the interference images are 280 µm in diameter as represented in the first image of BO + ZDDP + TDP(2C) lubricated ball surface

4.2 Friction

 Figure 3 shows the friction behaviour of the different lubricant formulations. As can be seen in **Figure 3**(b), at the start of the test (at which the tribofilm has not yet formed) the initial Stribeck curve of the BO + ZDDP was similar to that of the base oil. However; the effect of ZDDP was observed after only five minutes of rubbing and this results in the boundary/mixed condition being seen at higher intermediate speeds throughout the test. The development of ZDDP tribofilm on the contact surfaces causes a significant increase in the friction of the intermediate entrainment speeds as expected (23). The patchy nature of the ZDDP-tribofilm is known to inhibit the fluid-oil entrainment to the contact and enhances friction (22, 23, 26).

The Stribeck curve measured for BO+ZDDP after thirty minutes of rubbing remained similar until the end of the test implying that the tribofilm morphology, thickness and rate of microscopic-tribofilm formation and removal reached a steady state condition.
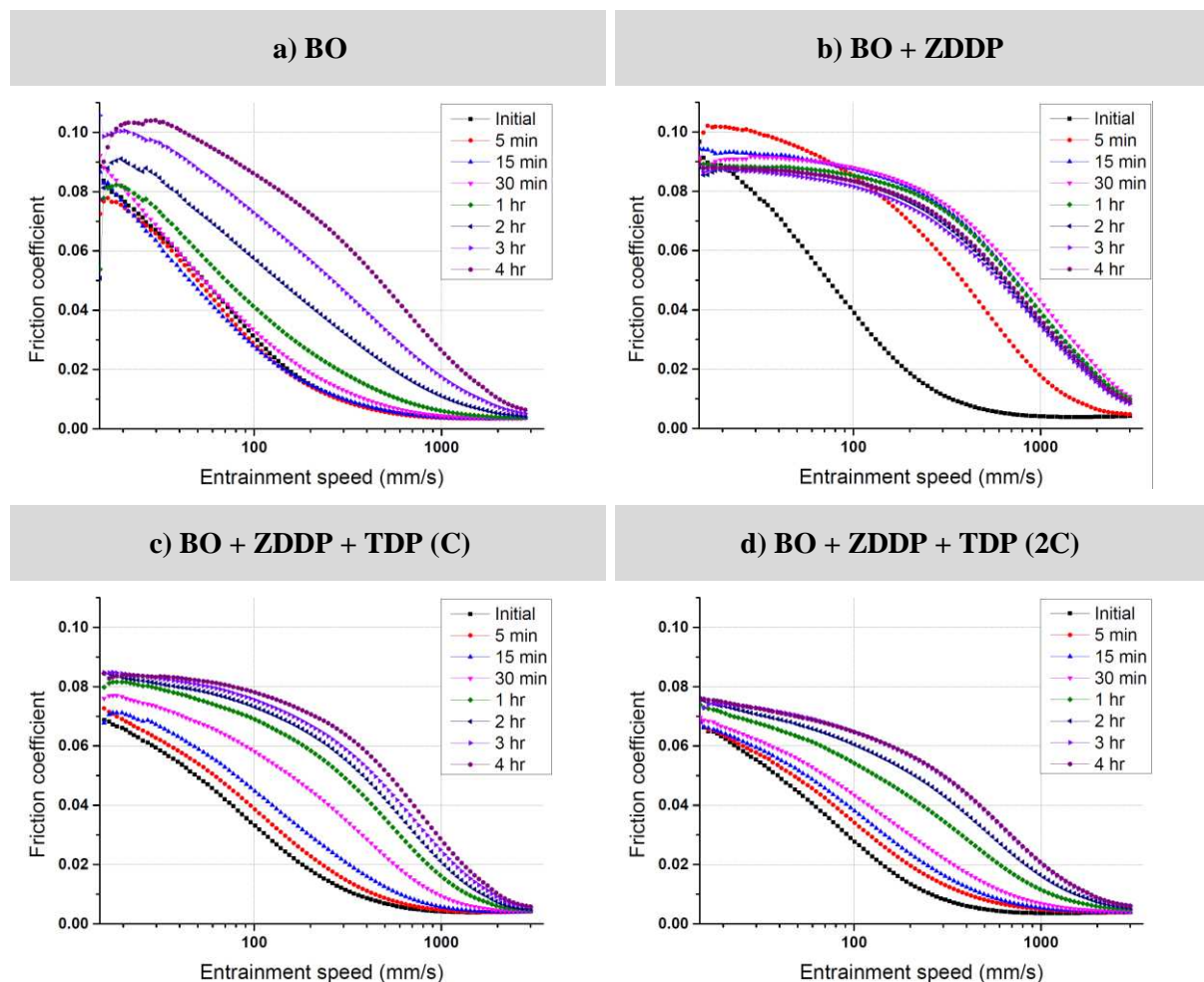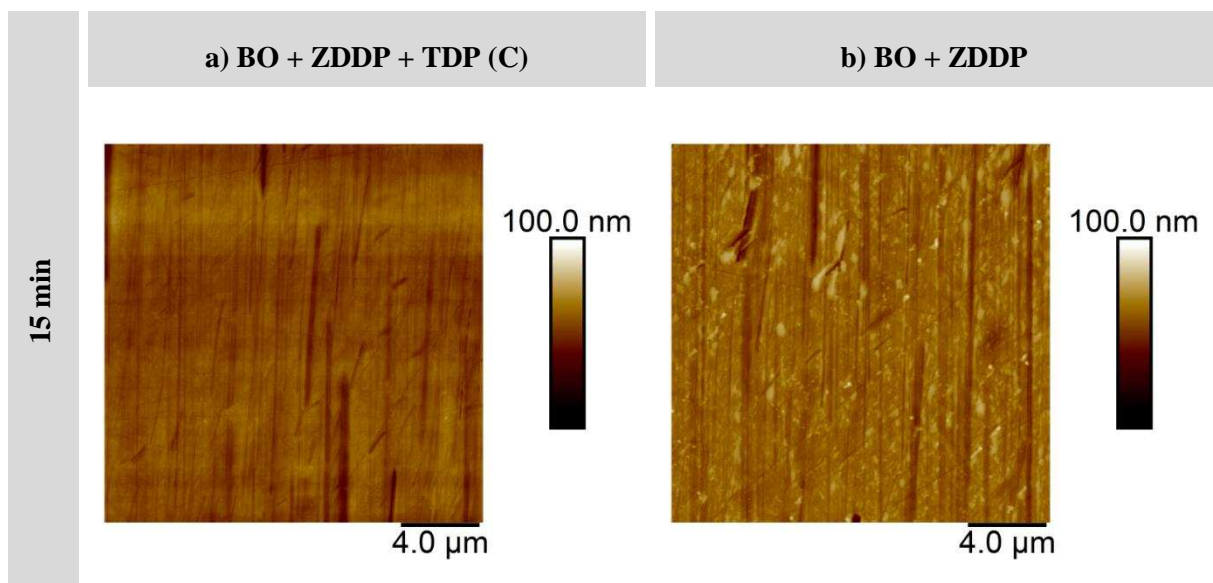

Figure 3. Stribeck diagrams measured after certain rubbing times for the four lubricant formulations

It can be noted that the Stribeck friction results for the BO test (**Figure 3** (a)) increases after each rubbing step continuously, caused by the wear process which roughens the surfaces. As shown in **Figure 3** (c and d), TDP in the lubricant decreases the boundary friction at the start of test compared to the BO and BO+ZDDP tests which can be attributed to the adsorbed film on the steel surfaces. Also, TDP reduced friction in the intermediate speed range (200 -1000 mm/s) throughout the test. A clear increase in friction occurred as soon as the tribofilm started to appear after 30 minutes and 1 hour of rubbing at TDP concentration of C and 2C respectively. After the first hour of rubbing, the friction coefficient during each traction step remains constant followed by an increase during Stribeck friction step due to the further tribofilm formation and mild wear.

Increasing the concentration of TDP from C to 2C led to more extensive friction reduction and delay of the tribofilm formation, probably due to greater TDP-ZDDP interactions and less ZDDP adsorption on the surface. In conclusion, TDP delays the ZDDP-derived tribofilm formation and supresses the ZDDP tribofilm friction-intensifying properties. MTM results showed that TDP in Oil-C and Oil-D reduced the friction coefficient in boundary and even more in mixed lubriction regime.

4.3 Topographical analysis of the tribofilms

AFM images have been taken on the tribofilms formed on the MTM discs at the approximate centre of the wear tracks. **Figure 4** and **Figure 5** show representative AFM images of 20×20 μm^2 area of the tribofilm.

c) Height profile of the tribofilm across the centre of the image (a)	d) Height profile of the tribofilm across the centre of the image (b)

$R_{rms} = 3.2$ nm
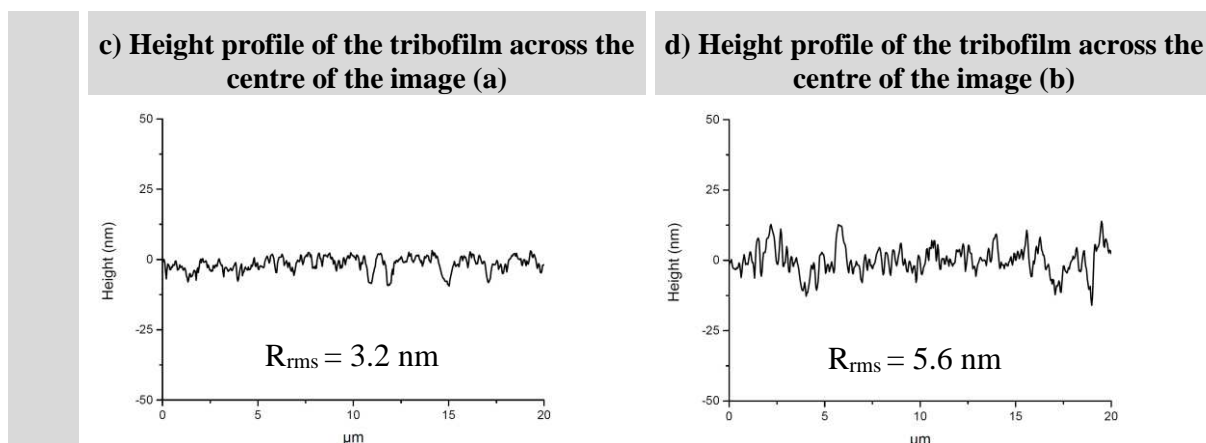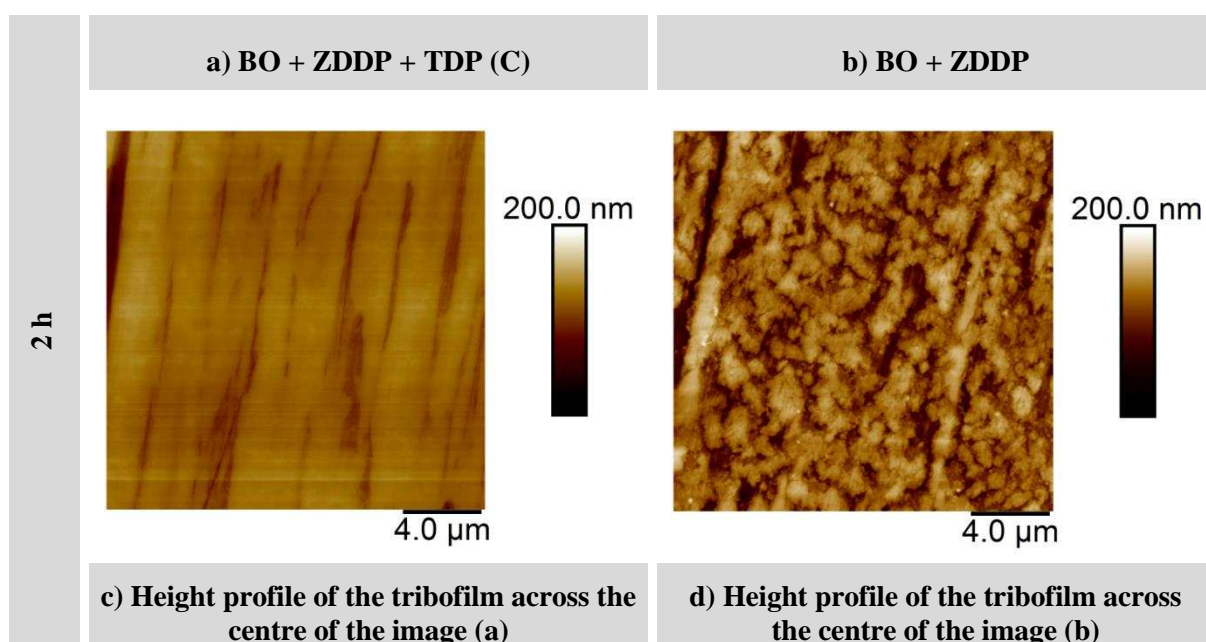

$R_{rms} = 5.6$ nm

Figure 4 AFM images and representative height-profiles across centre of the tribofilms induced after 15 minutes of rubbing in BO +ZDDP + TDP(C) and BO + ZDDP lubricants

The line profile below each image corresponds to height profile (in Z direction) of each AFM image at the centre of the image horizontally including root mean square roughness (R_{rms}) of the line profile. The roughness values (R_q) of the tribofilms induced by BO+ZDDP are 5.1 nm and 23.3 nm, while roughness values of the tribofilms induced by BO+ZDDP+TDP(C) are 3.9 nm and 12.5 nm after 15 minutes and 2 hours of rubbing respectively.

Smoother tribofilms are formed when TDP is present in the lubricant formulation. Representative AFM images of 5×5 µm^2 area of the tribofilm generated after two hours of rubbing are shown in **Figure 6**. The images show the patchy and uneven nature of the ZDDP-derived tribofilm; such a structure is well-established in the literature (27).

2 h

a) BO + ZDDP + TDP (C)	b) BO + ZDDP

200.0 nm

4.0 µm

200.0 nm

4.0 µm

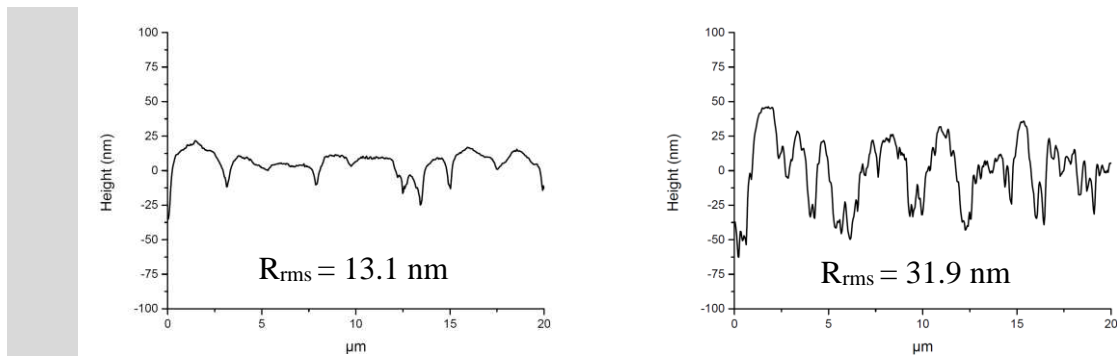| c) Height profile of the tribofilm across the centre of the image (a)	d) Height profile of the tribofilm across the centre of the image (b)

Figure 5. AFM images and representative height-profiles across centre of the tribofilms induced after 2 hours of rubbing in BO +ZDDP + TDP(C) and BO + ZDDP lubricants

In contrast to the tribofilm generated using BO+ZDDP, the tribofilm formed on the surface lubricated with BO+ZDDP+TDP(C) appeared to be smooth and seems to consist of evenly distributed pads along the sliding-rolling direction.
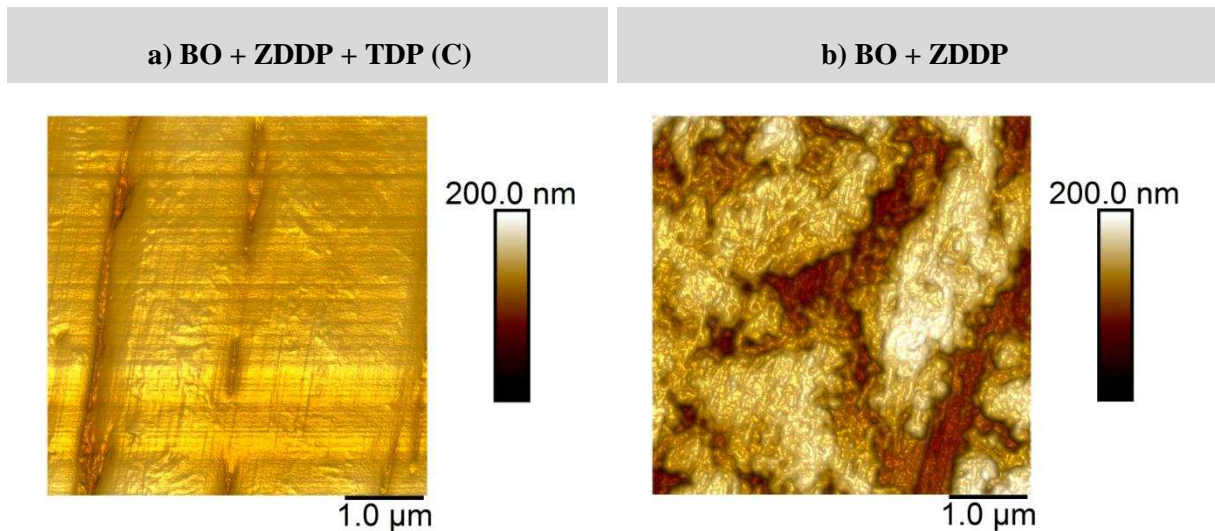
Figure 6. AFM images of the tribofilms induced after 2 hours of rubbing in a) BO +ZDDP + TDP(C) and b) BO + ZDDP lubricants

4.4 Micropitting results

4.4.1 Optical micrographs

As can be seen in **Figure 7**, on the surface of the roller lubricated with BO there is no visible micropitting since the dominant surface damage is wear. However, severe micropitting features are clearly observable on the roller lubricated with BO + ZDDP mostly appearing in the contact zone where the contact pressure is higher.

The micropitting-enhancing properties of the ZDDP-tribofilm shown in **Figure 7** is in agreement with previous reports (4, 21). Addition of TDP to the lubricant formulation

significantly reduced the micropitting features on the roller surfaces as can be seen in **Figure 7**.

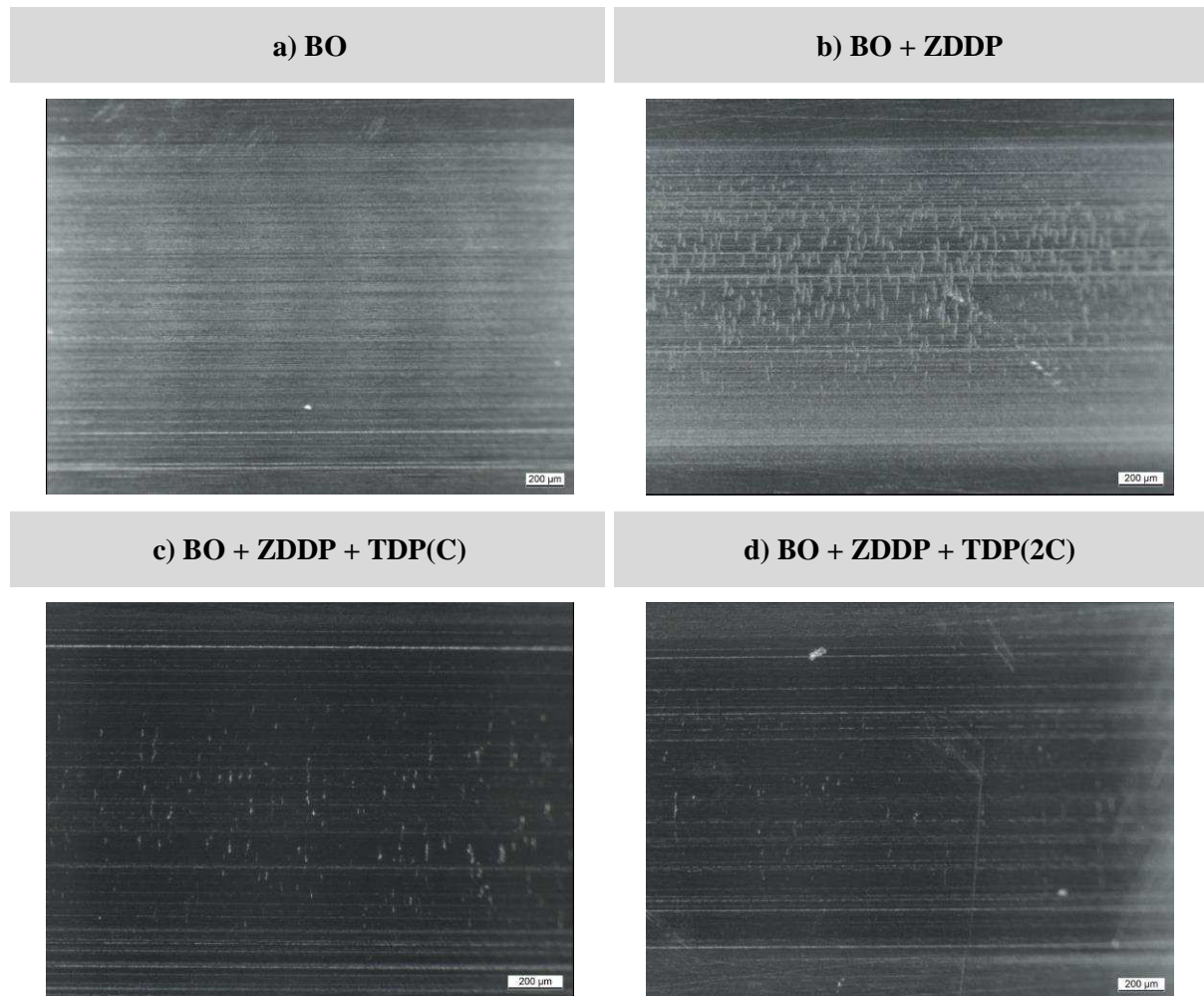| a) BO	b) BO + ZDDP
c) BO + ZDDP + TDP(C)	d) BO + ZDDP + TDP(2C)

Figure 7. Optical micrographs of the roller surfaces lubricated with a) BO, b) BO + ZDDP, c) BO + ZDDP + TDP(C), and d) BO + ZDDP + TDP(2C) lubricant formulations

4.4.2 SEM

In order to inspect micropitting in the wear scars and corresponding tribofilms, Secondary Electron (SE) images of the roller surfaces are taken using a low acceleration voltage (5KV). **Figure 8**(a and c) shows an extensively cracked surface and ruptured tribofilm perpendicular to the rolling direction on the roller lubricated with BO + ZDDP. This corresponds to micropitting generated beneath the tribofilm. The generated micropits propagate perpendicular to the rolling/sliding direction. On the right hand-side (**Figure 8**(b and d)) SE images of the roller lubricated with BO + ZDDP + TDP(2C) are shown, it is clear that the surface and tribofilm are more uniform and significantly more intact which is an indication of a surface with less micropitting surface density. High magnification images (**Figure 8** (c and d)) compare

a crack size on the roller surfaces. It is clear that the surface of the roller lubricated with BO+ZDDP+TDP(2C) is less cracked relative to that of the BO+ZDDP test surface. The more intact surface (and tribofilm) of BO+ZDDP+TDP(2C) probably results from smother tribofilm formed and its chemical composition.
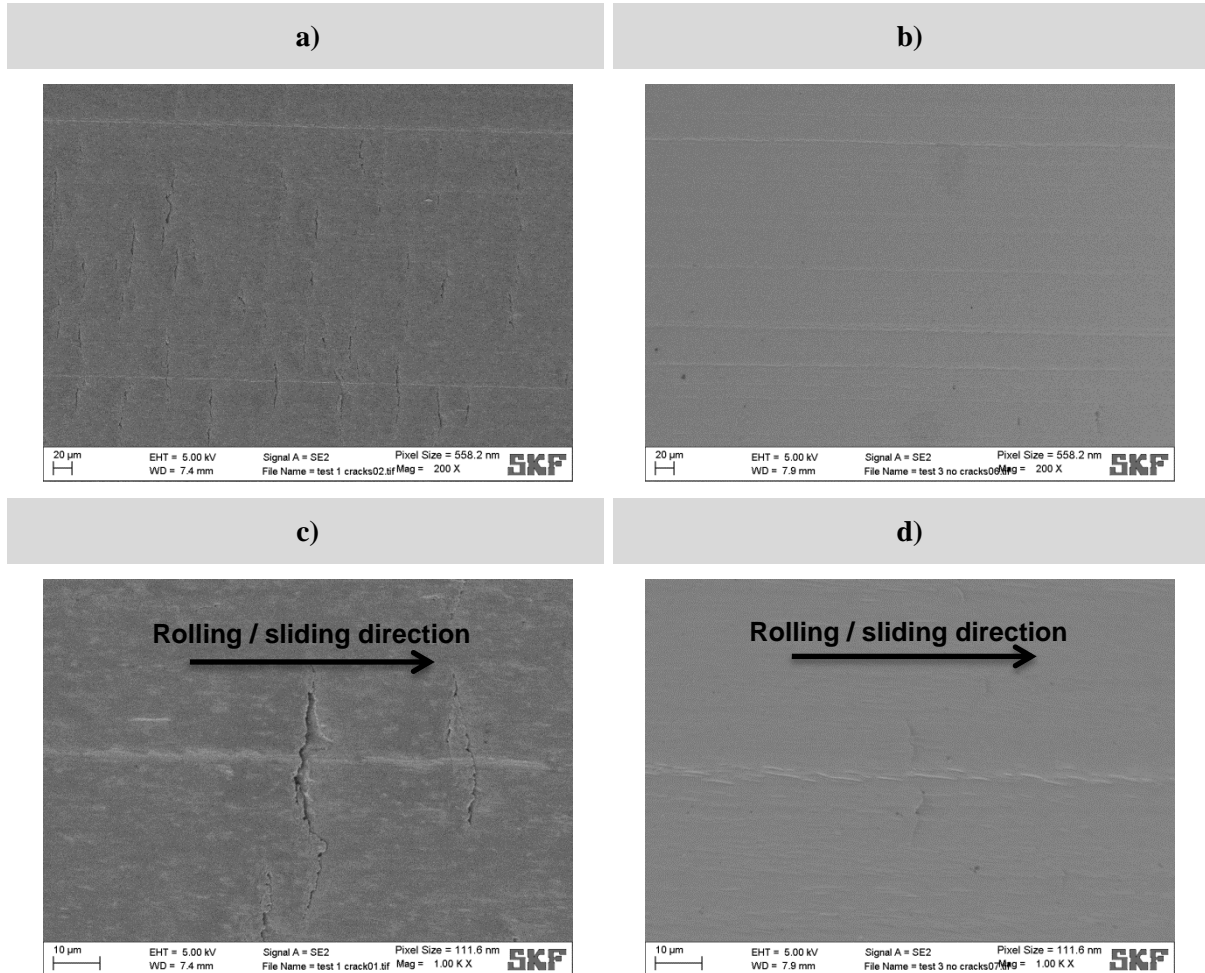
Figure 8. SEM images of the tribofilms on the roller surfaces lubricated with a and c) BO + ZDDP, b and d) BO + ZDDP + TDP (2C)

4.4.3 Wear track profile

In **Figure 9**, the deep wear profile of the roller lubricated with base oil indicates that the roller had undergone substantial material loss, while the roller lubricated with BO + ZDDP suffered severe micropitting on the surface. The wear profiles of the rollers lubricated with TDP-containing lubricant formulations clearly show considerably less micropitting on the surfaces compared to the roller lubricated with BO + ZDDP while rollers are protected from significant material loss observed with base oil formulation. Abrasive marks also can be seen on the rollers lubricated with TDP-containing lubricant formulations.

a) BO	c) BO + ZDDP + TDP (C)

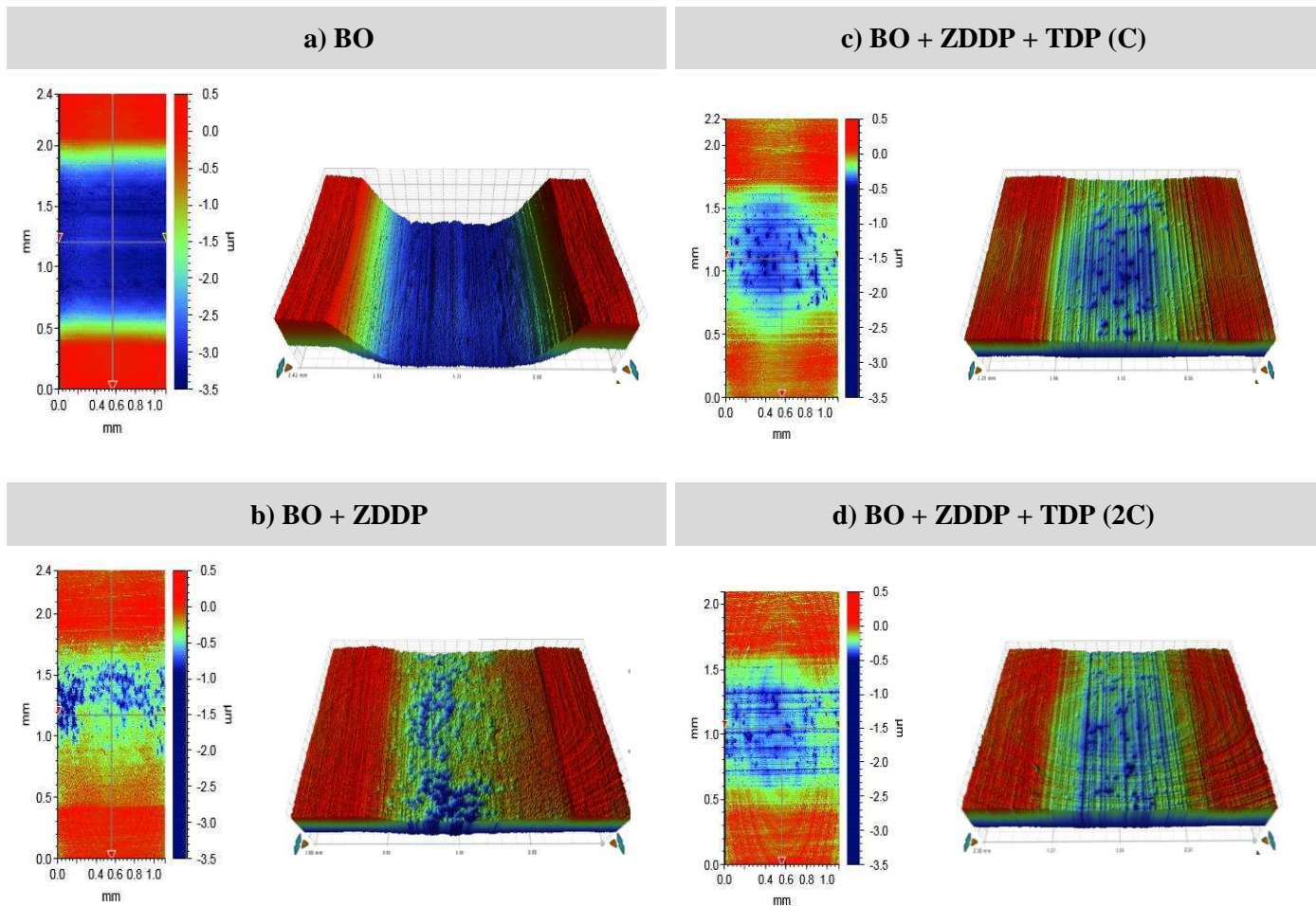| b) BO + ZDDP	d) BO + ZDDP + TDP (2C)

Figure 9. White light interferometric wear track profiles of the roller surfaces lubricated with a) BO, b) BO + ZDDP, c) BO + ZDDP + TDP (C), d) BO + ZDDP + TDP (2C)

4.4.4 Wear volume results

The total wear volume of the rollers lubricated with the different lubricant formulations is shown in **Figure 10**. Utilising ZDDP in the lubricant formulation reduces the wear volume by approximately 90% compared to the base oil alone as expected. Also, **Figure 10** shows that the addition of TDP to the BO+ZDDP reduces the total wear volume. For the lubricant formulations comprising TDP, a decrease of approximately 15% in wear volume was observed compared to BO + ZDDP formulation. **Figure 9** and **Figure 10** show that BO+ZDDP+TDP formulation significantly reduces the micropitting on the roller surface compared to BO+ZDDP formulation and protects the surface from wear more effectively than BO+ZDDP at the same time.

It should be noted that there are some reports (14, 26) addressing the antagonistic effect of amine-based additives on ZDDP and consequent increases in wear. These tests were carried out in different test conditions using a sliding high-frequency reciprocating rig (HFRR) and

valve train test. The test conditions in this study are mainly of interest to roller bearing applications and so are different to the previous reports (26). Also, the detrimental effect of amine-based additives is strongly dependent on the concentration and alkyl chain length (carbon number); as an example, addition of 2-ethylhexylamine to i-C3 ZDDP at molar ratio of 1:1 did not affect wear (14, 15, 18).
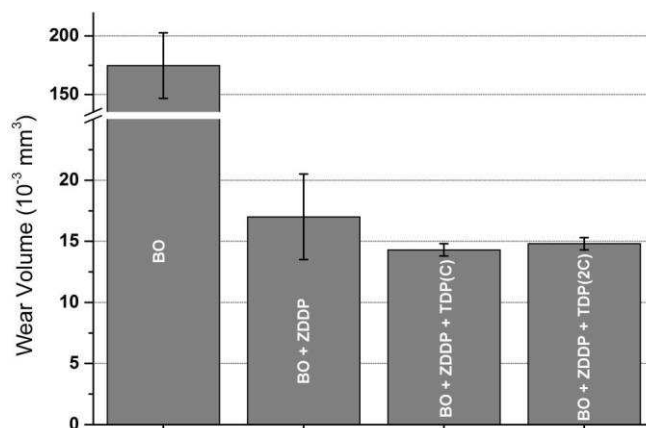

Figure 10. Total wear volumes occurred on the roller surfaces lubricated with the four lubricant formulations

4.5 Chemical composition of the tribofilms

XPS is employed to understand how the tribochemistry affects the changes in friction and micropitting wear seen when TDP is used in conjunction with ZDDP. The binding energies of the peaks and corresponding chemical compounds are summarised in **Table 5**.

The carbon C 1s spectra in the tribofilms are resolved to four peaks. The main peaks in both tribofilms appeared at 285.0 eV assigned to aliphatic carbon (C-C and C-H). The other three minor contributions in Oil-B were observed at 286.4, 287.6 and 289.0 ± 0.1 eV assigned to C-O, C-S and C=O (carbonate and/or carboxylic), respectively. Also, other three minor contributions in Oil-C appeared at 286.3, 287.7 and 288.8 ± 0.1 eV corresponding to C-O/C-N, C-S and C=O, respectively.

The O 1s signal consists of two peaks in Oil-B and three peaks in Oil-C (see **Figure 11**). The most intense peaks at 531.4 ± 0.1 eV (Oil-B) and 531.2 ± 0.1 eV (Oil-C) are assigned to Non-Bridging Oxygen (NBO) originated from the phosphate chain (-P=O and P-O-M; where M is metal: Zn or Fe), nitrates (Oil-C) (28), hydroxide and carbonates (Oil-B and Oil-C). The peaks at 532.9 ± 0.1 eV (Oil-B and Oil-C) correspond to Bridging Oxygen (BO) from phosphate chain (P-O-P) and sulphates in Oil-C. The peak at 529.8 eV ± 0.1 eV in the O 1s signal of Oil-C is attributed to the oxide.

The values of the P $2p_{3/2}$ peaks (133.3 ± 0.1 eV and 133.0 ± 0.1 eV for Oil-B and Oil-C, respectively) indicate that the top measured layer of the tribofilm is not expected to consist of long (poly)phosphate chains, since P $2p_{3/2}$ in the pure long chain zinc polyphosphate appears at 134-135 eV (29-32). A peak originating from Zn 3s was detected at 140.2 ± 0.1 eV (Oil-B) (139.9 ± 0.1 eV (Oil-C)) which is considered to calculate the quantification data, since the inelastic mean free path value of this peak is approximately same as that of the phosphorus signal and similar to those of the oxygen and sulphur signals (25, 33, 34).
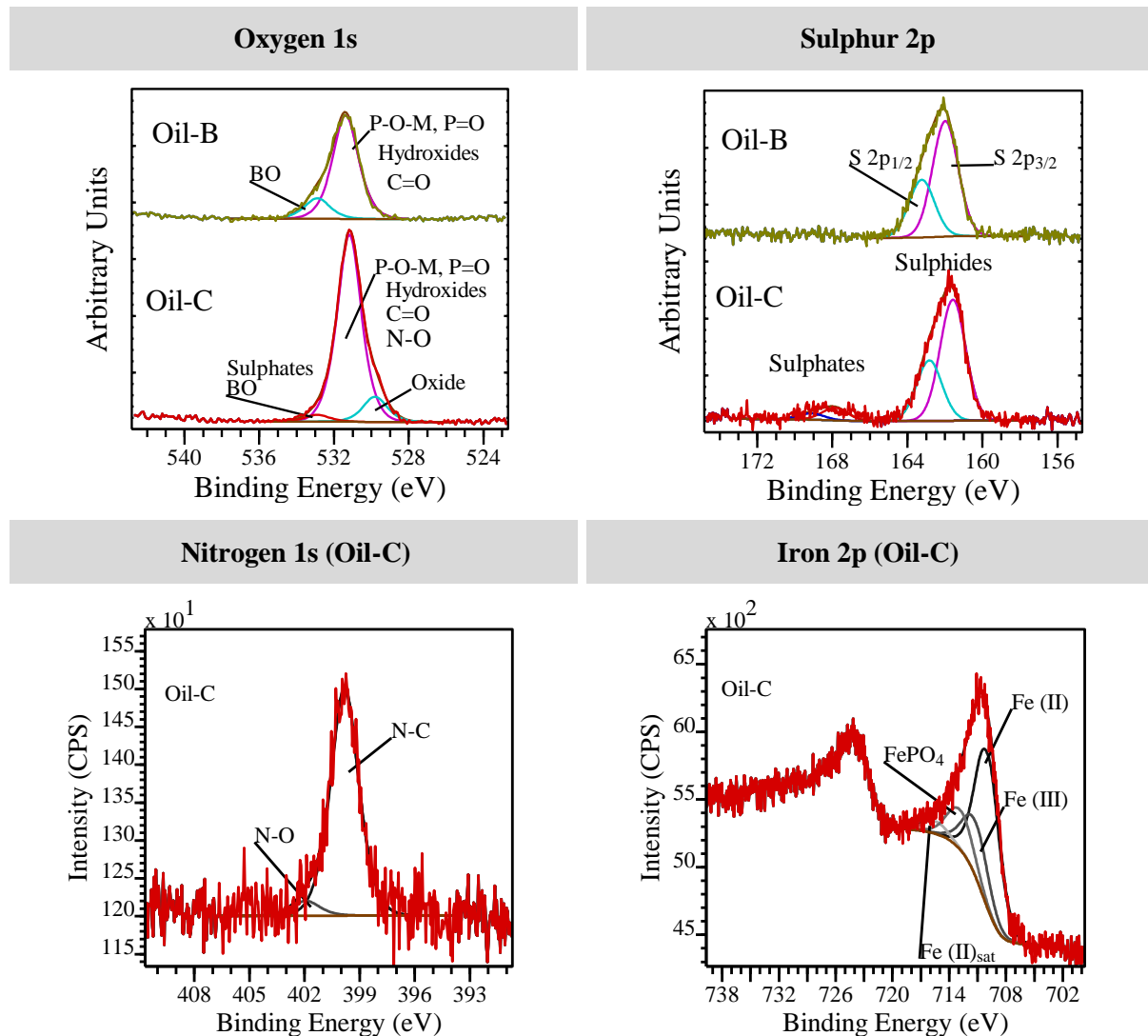
Figure 11. Detailed XPS spectra collected from MPR rollers in contact against rough rings lubricated with BO + ZDDP and BO + ZDDP + TDP (C) lubricant formulations

The contribution of nitrogen can be observed only in the spectra of the tribofilm on the roller lubricated with Oil-C. N 1s signal due to the lack of specific standards and a low signal to noise ratio is difficult to interpret. However, as shown in **Figure 11**, a peak can be resolved at 399.8 ± 0.1 eV that can be attributed to the N-C bond in the TDP additive. This N-C bond can be assigned to the adsorbed TDP on the surface or compound(s) of ZDDP and TDP interaction. A

minor peaks was also detected at 401.9 eV in N 1s signal which can be attributed to the N-O bond and/or ionized organic (di)amine (35). No trace of nitrogen was detected after 60 s of ion sputtering the reaction layer, suggesting that TDP does not contribute to the chemical composition of the bulk of the tribofilm.

As shown in **Figure 11**, the S 2p spectra from the tribofilms have signal in the oxidation state of -2 (SII) assigned to sulphides (36) as metal sulphide (ZnS) which are embedded precipitates and sulphur which is substituted for oxygen in the phosphate chain forming (polythio)phosphate (37). Using XPS is not easy to distinguish between (thio)phosphate and metal sulphide. A contribution of sulphate from sulphur (S 2p) in oxidation state of +6 (SVI) (36) was observed for the roller lubricated with Oil-C, generating a S $2p_{3/2}$ peak at 167.9 ± 0.1 eV. Sulphate is present on the top layer of the tribofilm and in the bulk of the tribofilm sulphide exists. The role of sulphate as an oxidised species is not thoroughly understood; however it is claimed to appear in thermally-decomposed ZDDP at outside of the wear track and at inside of the wear track of the boundary lubricated contact where the oil was contaminated with water (25, 38) or if an S-containing additive is used in the lubricant formulation (39). Sulphate contribution to the ZDDP-tribofilm in the wear track has also been shown using X-ray absorption near edge structure (XANES) spectroscopy (40) and XPS (41).

While an iron signal was not detected in Oil-B, iron (Fe 2p) signal in Oil-C was resolved to four peaks shown in **Figure 11**. Peaks at 709.9 ± 0.1 eV and 711.1 ± 0.1 eV can be attributed to iron oxide in oxidation states of +2 and +3, respectively. Oxide peak at 529.8 ± 0.1 eV in the O 1s signal can be attributed to the iron oxide accordingly. In addition, the peak at 712.8 ± 0.1 eV, attributed to $FePO_4$, suggests the contribution of iron to the (poly)phosphates in the tribofilm.

The polyphosphate chain length of the ZDDP-derived tribofilm is reported to have an important impact on its anti-wear performance (42). The BO/NBO ratio which has been used to evaluate the chain length of zinc phosphate glasses (42) may easily be affected by contaminants. Also, peaks can overlap with other components. Hydroxides and C=O (carbonyl and carbonate) can contribute to NBO peak (25, 28). Also, sulphate and P-O-C components (43) can contribute to the BO peak. Furthermore, the adsorbed water at 533.3-534.3 eV (28, 44) can bring about errors in the BO/NBO ratio. As a result, considering BO/NBO ratio for phosphate chain length estimation may bring about uncertainties. Therefore, complementary parameters are required to confirm the change in chain length.

Table 5. Binding energy values for the elements/compounds of the tribofilms and atomic concentrations of the tribofilm elements (Zn, S, O, and N) normalised to P

			BO + ZDDP	BO + ZDDP + TDP(c)
Binding energy (eV)	O 1s	BO	532.9 (83.3%)	532.9 (3.1%)
		NBO	531.4 (16.7%)	531.2 (85.4%)
		Oxide	-	529.8 (11.5%)
	P 2p$_{3/2}$ (eV)		133.3	133.0
	Zn 3s (eV)		140.2	139.9
	S 2p$_{3/2}$ (eV)	Sulphide	162.0	161.6 (84%)
		Sulphate	-	167.9 (16%)
	N 1s		-	399.8 (N-C) (93.8%)
			-	401.9 (N-O) (6.2%)
	Fe 2p$_{3/2}$	Fe (II)	-	Fe (II): 709.9 / Fe (II)$_{Sat}$: 715.4 62.3 %
		Fe (III)	-	711.1 (21.8%)
		FePO$_4$	-	712.8 (15.9%)
Atomic concentration ratio	BO/NBO ratio		0.20	0.04
	Zn/P		1.1	1.3
	S$_{II}$/P		0.6	0.6
	O$_{Phosphate}$/P		1.9	3.1
	N/P		-	0.2

A higher ratio of Zn/P together with an increase in the O/P ratio in the zinc phosphate chain suggests having greater ZnO/P$_2$O$_5$ mole fraction. In general with the more metal oxide fraction (shorter phosphate chain length), lower BO/NBO ratios and shift of P 2p$_{3/2}$ binding energy to lower value have been observed (44-47). In addition, in iron phosphate tribofilms, phosphate chains with lower Fe/P ratios consist of longer chains (43).

The BO/NBO ratio of almost zero together with low binding energy of the P 2p$_{3/2}$ peak (133.0 eV) in Oil-C suggests short chain phosphate formation in favour of pyro/ortho-phosphate. In addition, the decrease in BO/NBO ratio and binding energy of the P 2p$_{3/2}$ peak alongside the increase in Zn/P and O/P ratios in tribofilm of Oil-C infers shorter (polythio)phosphate chain development compared to the phosphate chain length in the tribofilm of Oil-B. This is in agreement with the Willermet et al. work (48, 49). Dispersants, which have polyamine in the chemical structure, in oil have been addressed to decrease the (poly)phosphate chain length in the ZDDP thermal-film (16) and tribofilm (17).

The cross-sectional schematics of the tribofilms are presented in **Figure 12** based on the XPS detailed spectra and sputtered profiles.

The sputtered profile of the tribofilm shown in **Figure 13**(a) confirms a thick tribofilm formation on the surface, since after 30 minutes of etching there is a substantial proportion of the tribofilm consists of P, S and Zn elements.
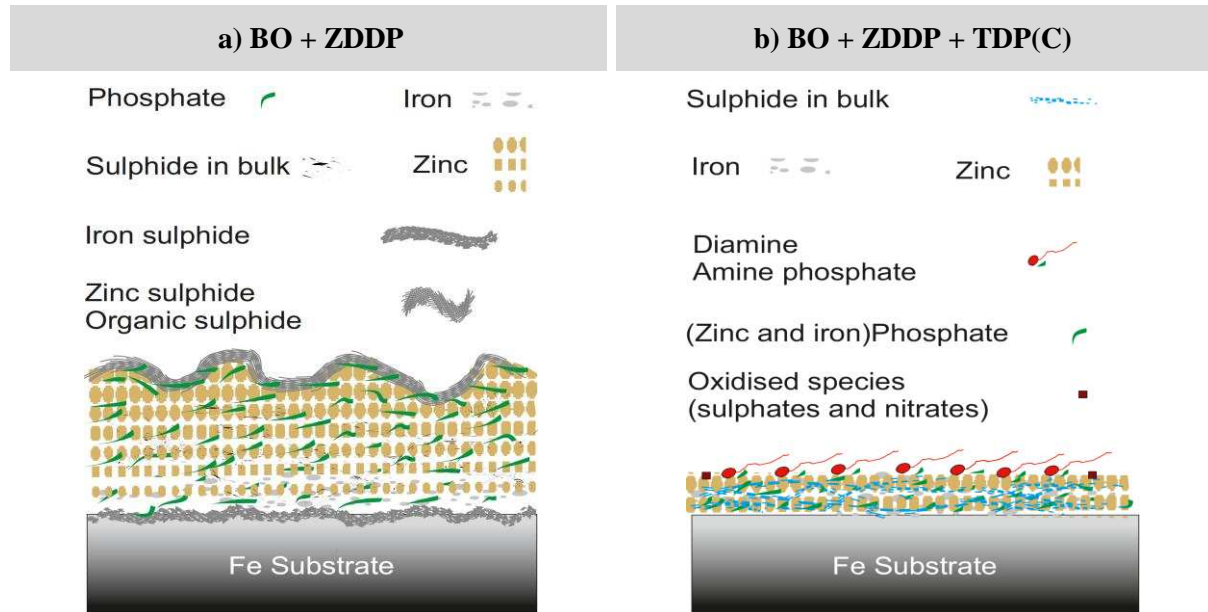

Figure 12. Schematic illustration of the tribofilms formed on the MPR roller surfaces lubricated with a) BO + ZDDP b) BO + ZDDP + TDP(C)

Iron does not appear until nine minutes of etching implying the existence of zinc (polythio)phosphate alongside sulphides (ZnS and/or species in the form of (polythio)phosphate) on the upper layer of the tribofilm. This is represented in **Figure 12** (a) that shows a decrease in the zinc concentration from top layer to the bulk and a decrease in the iron concentration from the substrate to the area close to the substrate. Relative S to P, O and Zn atomic ratios are larger in the top layer compared to the bulk of the tribofilm indicating an enhanced contribution of sulphides to the top layer of the tribofilm (see **Figure 12**(a)). Iron sulphide formation is expected on the substrate due to the very severe lubrication regime (37, 50). Carbon was not detected in the bulk of tribofilm generated from Oil-B confirming the inorganic nature of the ZDDP tribofilm (27, 48, 51).

A schematic illustration of the tribofilm induced by Oil-C is shown in **Figure 12**(b). The detected Fe signal in the spectra collected from the tribofilm formed from Oil-C (**Figure 11**) is an indication of a thinner tribofilm formation (51). This is confirmed through etching the tribofilm, by which, after only four minutes of etching (**Figure 13**(b)), no trace of tribofilm elements (P, Zn, and S) was observed. Thinner tribofilm formation on the roller surface can be due to less shear-resistant tribofilm induced by TDP, or due to the development of an inferior extent of tribofilm-precursors (28) on the top layer to compensate the removed tribofilm in the severe condition (52). The tribofilm consists of thin short chain mixed Fe/Zn (thio)phosphates

(pyro/ortho-phosphate) with a minor contribution of TDP residuals and oxidised species (sulphates and nitrates) on the top layer. Also, formation of (di)amine and phosphate compounds, possibly (di)amine phosphate (39), can be suggested on the top layer of the tribofilm considering the shifts of the NBO peak in the O 1s signal and P $2p_{3/2}$ peak in Oil-C spectra to lower binding energies with respect to the NBO and P $2p_{3/2}$ peaks in Oil-B spectra (shown in **Table 5**).
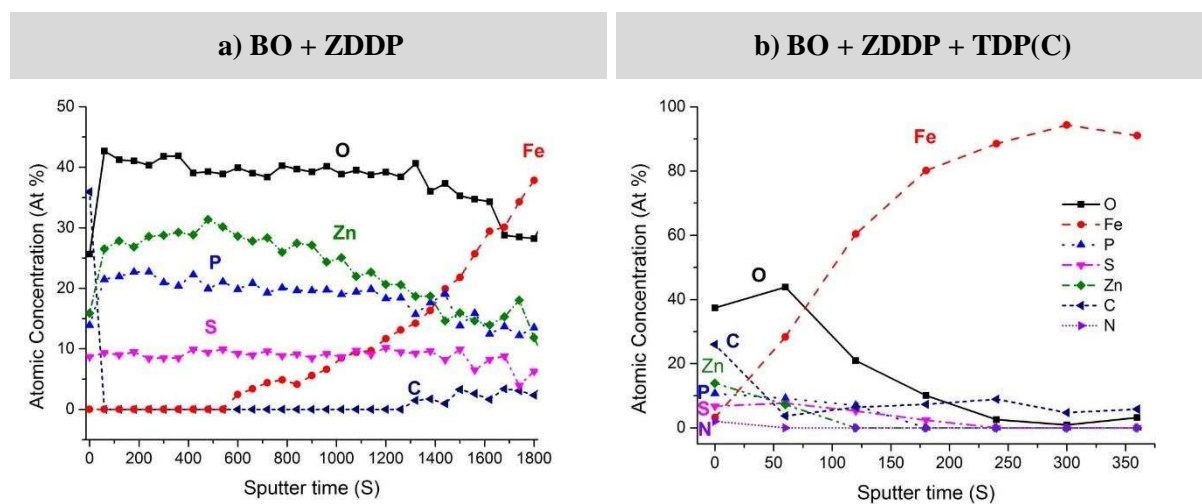

Figure 13. Sputter depth profiles of the reaction layers on the roller surfaces lubricated with a) BO + ZDDP and b) BO + ZDDP + TDP(C)

The contribution of ammonium phosphate (16, 17) or/and amine phosphate (53) to the phosphate chains in tribofilms induced by lubricants containing ZDDP and dispersants has been reported using XANES spectroscopy and XPS (39). The amine phosphate is formed through reaction of the pyrolytically dissociated amine group and decomposed ZDDP (53). This may imply the minor contribution of the TDP to the phosphate chain as (di)amine phosphate.

In comparison to the tribofilm formed from Oil-B, S/P atomic concentration ratio in the tribofilm bulk is enhanced in the tribofilm generated from Oil-C (comparing **Figure 12** (a) and (b)) showing greater sulphide contribution to the tribofilm bulk. Also, the relative concentration of the oxygen-to-phosphorous is enhanced in tribofilm from Oil-C on the top layer (O/P: 3.1) and in the bulk compared to the relative concentration in the tribofilm from Oil-B on top layer (O/P: 1.9) and in the bulk. This is in agreement with Pasaribu et al. (54) results showing superior rolling contact fatigue performances of the reaction layers having higher concentrations of oxygen rather than phosphorous.

5. Discussion

5.1 Effect of TDP on ZDDP tribofilm structure

The experiments were carried out utilising two test rigs; namely MTM and modified-MPR both in dominantly rolling conditions rather than sliding. Experimental and analytical results showed that TDP delays the tribofilm formation probably due to previously reported (14, 15, 18, 20, 28) acid-base interactions leading to complex formation or hydrogen bonding of nitrogen to phosphorous in ZDDP/ZDDP decomposition species (12, 13) hindering chemisorption. The tribofilms formed in the TDP-containing lubricants are approximately 20 nm thick on the MTM ball and MPR roller surfaces. Nevertheless, BO+ZDDP lubricant generates tribofilms in the order of 90 nm in thickness on the specimen's surfaces.

In this study, a thin mixed Zn/Fe short-chain (poly)phosphate has been observed to form on the roller surface lubricated with Oil-C. A lower BO/NBO ratio (42) and a lower P $2p_{3/2}$ binding energy (44, 47) together with greater cation concentration (16, 42) (Zn^{2+}, Fe^{3+}, and ionized amine) suggest shorter (poly)phosphates in the tribofilm from Oil-C compared to (poly)phosphates in the tribofilm from Oil-B. Also, metal or/and organic sulphides together with small portion of TDP residuals and oxidised species (sulphates and nitrates) were detected on the top layer of the tribofilm. A minor contribution of the (ionized)-(di)amine phosphate to the tribofilm can be suggested on the very top surface. Greater sulphide and oxygen concentrations in the bulk of the tribofilm have been observed which may bring about greater rolling contact fatigue life (54). However; the tribofilm on the roller lubricated with BO+ZDDP is thick and consists of short chain zinc (poly)phosphates along with metal (Zn) or/and organic sulphides on the top layer.

AFM results showed the smooth tribofilm formation and growth induced by TDP. The mechanism of the smooth tribofilm formation can be attributed to ZDDP and TDP interactions in the lubricant and consequently sustained chemisorption of the ZDDP-decomposition products.

5.2 TDP effect on friction and micropitting wear

The effect of ZDDP in increasing friction is reduced using TDP in lubricants. Friction reduction both in boundary and mixed entrainment speeds has been observed due to smoother tribofilm formation and adsorption of TDP or compounds formed through ZDDP and TDP interactions on the tribofilm and steel surface where no tribofilm is formed.

Shown in **Figure 9** (c and d), the abrasive marks in the wear tracks on the roller surfaces lubricated with Oil-C and Oil-D, can be explained by the hard and soft acids and bases (HSAB) theory which is established by Ho and Pearson (55, 56) and well-implemented to ZDDP by Martin (42). Based on this theory the thicker and longer-chain (poly)phosphate (hard base) can digest the iron-oxide wear particles (in comparison to zinc-oxide, iron-oxide is a harder Lewis acid) and avoid abrasive wear. The tribofilm resulted from TDP is thin (shown in **Figure 12**(b) and **Figure 13**(b)) and consists of short-chain (poly)phosphates; thus the abrasive marks can be expected.

SEM images of the rollers revealed extensively cracked surfaces (and tribofilm) of rollers lubricated with BO+ZDDP. The surfaces lubricated with TDP-containing lubricant are considerably less damaged. The optical microscopy together with WLI images showed the effective reduction in micropitting on MPR rollers using TDP in lubricant formulation. The total wear volumes are measured on the rollers, disclosing the rolling-wear reduction efficiency of TDP after a million of cycles when it is introduced to the lubricant formulation in combination with ZDDP. The surface of the roller undergoes less micropitting compared to BO+ZDDP while protected from wear happening on the roller lubricated with base oil.

As far as micropitting is concerned in a steel-steel contact, the most derivative to induce micropitting is the roughness difference between the surface and the counterpart (1, 7). However, the effect of ZDDP tribofilm on micropitting intensification may include further parameters.

The viscous soft top polyphosphate layer (57) can accommodate the rolling/sliding shear stress inside the tribofilm rather transferring this to the substrate surface (52), while short chain zinc (or mixed Fe/Zn) (poly)phosphates are believed to be stable and more shear resistant and has higher hardness compared to the soft polyphosphate layer (52) probably due to having higher Young's moduli values and accumulation of residual compressive stresses (27). While rubbing contact progresses, the tribofilm becomes thicker up to a certain time (58) and forms harder and shorter chain (poly)phosphate (37) which is expected to be more shear resistant. As a result lower viscous flows on the surface caused by harder short-chain metal-(poly)phosphates can be expected.

Alongside ZDDP early and fast decomposition on the surface, depolymerisation of the tribofilm to a harder and more shear-resistant zinc (or mixed Fe/Zn) short polyphosphate in the wear process may upsurge the micropitting incident through accumulation of local plastic

deformation. The early ZDDP-tribofilm formation hinders proper running-in of surfaces (1, 4, 27) consequently hinders the decline in roughness (1, 59). The depolymerisation of the ZDDP-tribofilm to a shear-resistant zinc (or mixed Fe/Zn) short polyphosphate in the wear process is expected due to iron-oxide digestion (42) or substrate iron ion diffusion to the tribofilm (27).

Thin together with smoother tribofilm formation induced by TDP+ZDDP formulation suggests less shear resistance nature of the tribofilm which may induce less local plastic deformation. The chemically modified tribofilm and smoother tribofilm formation accompanied with improved running-in process due to the delayed tribofilm (and chemisorbed film) formation suggested to be the reason behind micropitting and friction reduction capability of TDP+ZDDP formulation.

6. Conclusions

Experimental and analytical results showed that TDP, as an environmentally friendly organic additive, in combination with ZDDP effectively mitigates the micropitting-intensifying behavior of ZDDP while the surface is protected from wear. Furthermore, the rolling/sliding wear performance is comparatively improved using TDP in the lubricant formulation together with ZDDP compared to BO + ZDDP formulation in the test conditions used in this study. The following conclusions can also be drawn from this study:

- TDP reduces the friction-intensifying behavior of the ZDDP-containing oil and delays the tribofilm formation. Addition of TDP to the ZDDP-containing oil reduces the tribofilm thickness formed on the surface.

- The tribofilm formed on the MPR roller lubricated with base oil + ZDDP is composed of metal(zinc at top layer and zinc/iron in bulk) short chain (poly)phosphates and (metal and organic) sulphides. Tribofilm formed on the MPR roller lubricated with base oil + ZDDP + TDP is composed of mixed zinc and iron short chain (poly)phosphates, (metal and organic) sulphides and a minor extent of oxidised species (sulphates and nitrates). Traces of nitrogen from TDP molecule were detected only on the top layer of the tribofilm which can be attributed to the adsorbed TDP molecules and amine phosphates. TDP enhances the atomic ratios of S/P, O/P and O/S indicating a greater contribution of oxygen to the tribofilm.

- Using TDP-containing lubricant a smoother tribofilm was achieved. TDP inhibits patchy ZDDP-derived tribofilm formation. The micropitting and friction reduction, attained through adding TDP to the lubricant, is attributed to the smooth tribofilm formation

alongside the modified chemical structure of the tribofilm derived from base oil + ZDDP + TDP lubricant formulation.

7. Acknowledgments

8. References:

1.   Laine E, Olver A, Beveridge T. Effect of lubricants on micropitting and wear. Tribol Int. 2008;41(11):1049-55.

2.   Lainé E, Olver AV, Lekstrom MF, Shollock BA, Beveridge TA, Hua DY. The effect of a friction modifier additive on micropitting. Tribol Trans. 2009;52(4):526-33.

3.   O'connor B. The influence of additive chemistry on micropitting. Gear Technology. 2005;22(3):34-41.

4.   Brizmer V, Pasaribu H, Morales-Espejel GE. Micropitting performance of oil additives in lubricated rolling contacts. Tribol Trans. 2013;56(5):739-48.

5.   Brechot P, Cardis A, Murphy W, Theissen J. Micropitting resistant industrial gear oils with balanced performance. Ind Lubr Tribol. 2000;52(3):125-36.

6.   Johansson J, Devlin MT, Prakash B. Lubricant additives for improved pitting performance through a reduction of thin-film friction. Tribol Int. 2014;80:122-30.

7.   Berthe D, Flamand L, Foucher D, Godet M. Micropitting in Hertzian contacts. J Lubric Technol(Trans ASME). 1980;102(4):478-89.

8.   Brizmer V, Gabelli A, Vieillard C, Morales-Espejel G. An Experimental and Theoretical Study of Hybrid Bearing Micropitting Performance under Reduced Lubrication. Tribol Trans. 2015(just-accepted):00-.

9.   Akamatsu Y, Tsushima N, Goto T, Hibi K. Influence of surface roughness skewness on rolling contact fatigue life. Tribol Trans. 1992;35(4):745-50.

10.   Oila A, Bull S. Assessment of the factors influencing micropitting in rolling/sliding contacts. Wear. 2005;258(10):1510-24.

11.   Plaza S. The adsorption of zinc dibutyldithiophosphates on iron and iron oxide powders. ASLE transactions. 1987;30(2):233-40.

12.   Inoue K, Watanabe H. Interactions of engine oil additives. ASLE transactions. 1983;26(2):189-99.

13.   Gallopoulos NE, Murphy CK. Interactions between a zinc dialkylphosphorodithioate and lubricating oil dispersants. ASLE TRANSACTIONS. 1971;14(1):1-7.

14.   Shiomi M, Tokashiki M, Tomizawa H, Kuribayashi T. Interaction between zinc dialkyldithiophosphate and amine. Lubr Sci. 1989;1(2):131-47.

15.   Shiomi M, Mitsui Ji, Akiyama K, Tasaka K, Nakada M, Ohira H. Formulation Technology for Low Phosphorus Gasoline Engine Oils. SAE Technical Paper; 1992.

16.   Zhang Z, Kasrai M, Bancroft G, Yamaguchi E. Study of the interaction of ZDDP and dispersants using X-ray absorption near edge structure spectroscopy—part 1: thermal chemical reactions. Tribol Lett. 2003;15(4):377-84.

17.   Yamaguchi E, Zhang Z, Kasrai M, Bancroft G. Study of the interaction of ZDDP and dispersants using X-ray absorption near edge structure spectroscopy—part 2: tribochemical reactions. Tribol Lett. 2003;15(4):385-94.

18.   Rounds FG. Additive interactions and their effect on the performance of a zinc dialkyl dithiophosphate. Asle Transactions. 1978;21(2):91-101.

19.   Zhang J, Yamaguchi E, Spikes H. The antagonism between succinimide dispersants and a secondary zinc dialkyl dithiophosphate. Tribol Trans. 2014;57(1):57-65.

20.   Harrison PG, Brown P, McManus J. 31 P NMR study of the interaction of a commercial succinimide-type lubricating oil dispersant with zinc (II) bis (O, O'-di-iso-butyldithiophosphate). Wear. 1992;156(2):345-9.

21.   Morales-Espejel GE, Brizmer V. Micropitting modelling in rolling–sliding contacts: Application to rolling bearings. Tribol Trans. 2011;54(4):625-43.

22.   Taylor L, Dratva A, Spikes H. Friction and wear behavior of zinc dialkyldithiophosphate additive. Tribol Trans. 2000;43(3):469-79.

23.   Taylor L, Spikes H. Friction-enhancing properties of ZDDP antiwear additive: part I—friction and morphology of ZDDP reaction films. Tribol Trans. 2003;46(3):303-9.

24.   Hamrock BJ, Dowson D. Isothermal elastohydrodynamic lubrication of point contacts: Part III—Fully flooded results. J Tribol. 1977;99(2):264-75.

25.   Nedelcu I, Piras E, Rossi A, Pasaribu H. XPS analysis on the influence of water on the evolution of zinc dialkyldithiophosphate–derived reaction layer in lubricated rolling contacts. Surface and Interface Analysis. 2012;44(8):1219-24.

26.   Miklozic KT, Forbus TR, Spikes HA. Performance of friction modifiers on ZDDP-generated surfaces. Tribol Trans. 2007;50(3):328-35.

27.   Spikes H. The history and mechanisms of ZDDP. Tribol Lett. 2004;17(3):469-89.

28.   Martin J, Grossiord C, Le Mogne T, Igarashi J. Role of nitrogen in tribochemical interaction between Zndtp and succinimide in boundary lubrication. Tribol Int. 2000;33(7):453-9.

29. Onyiriuka E. Zinc phosphate glass surfaces studied by XPS. Journal of non-crystalline solids. 1993;163(3):268-73.

30. Brow RK, Tallant DR. Structural design of sealing glasses. Journal of Non-Crystalline Solids. 1997;222:396-406.

31. Eglin M, Rossi A, Spencer ND. X-ray photoelectron spectroscopy analysis of tribostressed samples in the presence of ZnDTP: a combinatorial approach. Tribol Lett. 2003;15(3):199-209.

32. Yin Z, Kasrai M, Bancroft G, Fyfe K, Colaianni M, Tan K. Application of soft X-ray absorption spectroscopy in chemical characterization of antiwear films generated by ZDDP Part II: the effect of detergents and dispersants. Wear. 1997;202(2):192-201.

33. Eglin M. Development of a combinatorial approach to lubricant additive characterization: Diss., Technische Wissenschaften ETH Zürich, Nr. 15054, 2003; 2003.

34. Seah M, Dench W. Quantitative electron spectroscopy of surfaces. Surface and interface analysis. 1979;1(1):2-11.

35. Matsumoto K. Surface chemical and tribological investigations of phosphorus-containing lubricant additives: Diss., Technische Wissenschaften ETH Zürich, Nr. 15150, 2003; 2003.

36. Brion D. Etude par spectroscopie de photoelectrons de la degradation superficielle de FeS 2, CuFeS 2, ZnS et PbS a l'air et dans l'eau. Applications of Surface Science. 1980;5(2):133-52.

37. Martin JM, Grossiord C, Le Mogne T, Bec S, Tonck A. The two-layer structure of Zndtp tribofilms: Part I: AES, XPS and XANES analyses. Tribol Int. 2001;34(8):523-30.

38. Cen H, Morina A, Neville A, Pasaribu R, Nedelcu I. Effect of water on ZDDP anti-wear performance and related tribochemistry in lubricated steel/steel pure sliding contacts. Tribol Int. 2012;56:47-57.

39. Komvopoulos K, Do V, Yamaguchi E, Yeh S, Ryason P. X-ray photoelectron spectroscopy analysis of antiwear tribofilms produced on boundary-lubricated steel surfaces from sulfur-and phosphorus-containing additives and metal deactivator additive. Tribol Trans. 2004;47(3):321-7.

40. Sharma V, Erdemir A, Aswath PB. An analytical study of tribofilms generated by the interaction of ashless antiwear additives with ZDDP using XANES and nano-indentation. Tribol Int. 2015;82:43-57.

41. Bell J, Delargy K, Seeney A. Paper IX (ii) The Removal of Substrate Material through Thick Zinc Dithiophosphate Anti-Wear Films. Tribology series. 1992;21:387-96.

42. Martin JM. Antiwear mechanisms of zinc dithiophosphate: a chemical hardness approach. Tribol Lett. 1999;6(1):1-8.

43. Rossi A, Piras F, Kim D, Gellman A, Spencer N. Surface reactivity of tributyl thiophosphate: effects of temperature and mechanical stress. Tribol Lett. 2006;23(3):197-208.

44.	Crobu M, Rossi A, Mangolini F, Spencer ND. Chain-length-identification strategy in zinc polyphosphate glasses by means of XPS and ToF-SIMS. Analytical and bioanalytical chemistry. 2012;403(5):1415-32.

45.	Liu H, Chin T, Yung S. FTIR and XPS studies of low-melting PbO-ZnO-P 2 O 2 glasses. Materials chemistry and physics. 1997;50(1):1-10.

46.	Crobu M, Rossi A, Mangolini F, Spencer ND. Tribochemistry of bulk zinc metaphosphate glasses. Tribol Lett. 2010;39(2):121-34.

47.	Heuberger RC. Combinatorial study of the tribochemistry of anti-wear lubricant additives: Diss., Eidgenössische Technische Hochschule ETH Zürich, Nr. 17207, 2007; 2007.

48.	Willermet P, Carter R, Boulos E. Lubricant-derived tribochemical films—an infra-red spectroscopic study. Tribol Int. 1992;25(6):371-80.

49.	Willermet P, Dailey D, Carter R, Schmitz P, Zhu W, Bell J, et al. The composition of lubricant-derived surface layers formed in a lubricated cam/tappet contact II. Effects of adding overbased detergent and dispersant to a simple ZDTP solution. Tribol Int. 1995;28(3):163-75.

50.	Minfray C, Martin J, Esnouf C, Le Mogne T, Kersting R, Hagenhoff B. A multi-technique approach of tribofilm characterisation. Thin Solid Films. 2004;447:272-7.

51.	Piras FM, Rossi A, Spencer ND. Combined in situ (ATR FT-IR) and ex situ (XPS) study of the ZnDTP-iron surface interaction. Tribol Lett. 2003;15(3):181-91.

52.	Bec S, Tonck A, Georges J-M, Coy R, Bell J, Roper G, editors. Relationship between mechanical properties and structures of zinc dithiophosphate anti–wear films. Proceedings of the Royal Society of London A: Mathematical, Physical and Engineering Sciences; 1999: The Royal Society.

53.	Zhang Z, Yamaguchi E, Kasrai M, Bancroft G. Interaction of ZDDP with borated dispersant using XANES and XPS. Tribol Trans. 2004;47(4):527-36.

54.	Pasaribu H, Lugt P. The composition of reaction layers on rolling bearings lubricated with gear oils and its correlation with rolling bearing performance. Tribol Trans. 2012;55(3):351-6.

55.	Ho T-L. Hard soft acids bases (HSAB) principle and organic chemistry. Chemical Reviews. 1975;75(1):1-20.

56.	Pearson RG. Chemical hardness: Wiley-VCH; 1997.

57.	Pidduck A, Smith G. Scanning probe microscopy of automotive anti-wear films. Wear. 1997;212(2):254-64.

58.	Fuller MS, Fernandez LR, Massoumi G, Lennard W, Kasrai M, Bancroft G. The use of X-ray absorption spectroscopy for monitoring the thickness of antiwear films from ZDDP. Tribol Lett. 2000;8(4):187-92.

59.	Benyajati C, Olver A, Hamer C. An experimental study of micropitting, using a new miniature test-rig. Tribology Series. 2003;43:601-10.